Available online at www.sciencedirect.com
ScienceDirect
Catalysis Today 118 (2006) 198–204
CATALYSIS TODAY
www.elsevier.com/locate/cattod

Preparation of Pt-loaded hydrogen selective membranes for methanol reforming

Dong-Wook Lee [a,b], Seung-Eun Nam [a], Bongkuk Sea [a], Son-Ki Ihm [b], Kew-Ho Lee [a,*]

[a] *Membrane and Separation Research Center, Korea Research Institute of Chemical Technology, P.O. Box 107, Yuseong, Daejeon 305-606, South Korea*

[b] *Department of Chemical and Biomolecular Engineering, National Research Laboratory for Environmental Catalysis, Korea Advanced Institute of Science and Technology, 373-1 Guseong-Dong, Yuseong-Gu, Daejeon 305-701, South Korea*

Available online 27 June 2006

Abstract

We prepared Pt-included microporous silica membranes (SiO_2/γ-Al_2O_3/Pt–SiO_2/porous stainless steel (SUS)) to improve CO removal efficiency in a methanol reforming membrane reactor. The permeation test of an H_2 (99%)/CO (1%) mixture between 25 and 200 °C was conducted to observe the effect of the Pt intermediate layer included in the membrane on CO removal efficiency. A mesoporous membrane with the Pt intermediate layer (γ-Al_2O_3/Pt–SiO_2/SUS) showed a remarkable H_2/CO separation factor of 5.22–7.03, exceeding the Knudsen-dominated transport characteristics expected from a mesoporous γ-Al_2O_3 layer. After coating a microporous silica skin layer on the Pt-included γ-Al_2O_3 membrane, CO was not detected in the permeate side of the membrane by the corona ionization detector (CID). When the Pt-included microporous silica membrane was used in the methanol reforming membrane reactor, methanol conversion at 200 °C (methanol/water feed flow rate = 0.004 ml/min) was improved from 73.2% to 93.2% in comparison with the case of a conventional reactor, and CO in the produced gas mixture was efficiently rejected through the Pt-included silica composite membrane. The introduction of the Pt catalyst into the intermediate layer of the composite membrane contributed to the improvement in CO removal efficiency. The dilution of CH_3OH/H_2O feed led to an increase in the extent of methanol conversion improvement (a difference of methanol conversion between a membrane reactor and a conventional reactor) due to an increase in the hydrogen recovery.

Keywords: Methanol reforming; CO removal; Membrane reactor

1. Introduction

Proton exchange membrane fuel cell (PEMFC) stacks are considered to be one of the most promising options as a substitute for the internal combustion engine for a number of transportation applications. The drive systems for cars using PEMFC can lead to increased energy usage efficiency and, especially, substantially reduced emissions compared with the best foreseeable drive system based on the internal combustion engine. Hydrogen as a fuel source for PEMFC can be economically produced by steam reforming of methanol or hydrocarbons such as natural gas, gasoline, and diesel fuel [1–3]. When hydrogen is obtained by hydrocarbon reforming, water–gas shift reactors of a significant size are needed owing to the large CO concentration produced at a high reaction temperature. In terms of processing temperature and CO contents, methanol steam reforming is considered to be a more suitable system for an energy carrier of PEMFC [4–6], because higher methanol conversion can be achieved at a low reaction temperature in the range of 250–350 °C, and products from methanol steam reforming contain CO of low concentration ranging from 1000 to 10,000 ppm [7,8].

However, the PEMFC anode feed gas should contain carbon monoxide (CO) less than 100 ppm and preferably less than 20 ppm, since the anode catalyst is usually based on platinum (Pt), which is easily poisoned by even a low concentration of CO. In order to diminish CO concentration in the anode feed gas, several physical and chemical purification methods, such as pressure swing adsorption (PSA), inorganic membranes, organic membranes, solvent absorption, water-gas shift reaction, methanation and preferential oxidation (PROX), have been studied. In addition, new electrocatalyst materials with a lower affinity for CO were investigated by several research groups [9–11].

In this paper, a Pt-loaded silica composite membrane has been used to reduce the CO concentration in the products of

* Corresponding author. Tel.: +82 42 860 7240; fax: +82 42 861 4151.
E-mail address: khlee@krict.re.kr (K.-H. Lee).

0920-5861/$ – see front matter
doi:10.1016/j.cattod.2005.12.005

methanol steam reforming as an energy carrier of PEMFC. A number of research groups have reported hydrogen-selective silica composite membranes derived from the sol–gel method [12–17]. For the methanol reforming membrane reactor, we fabricated a silica composite membrane supported on a Pt/SiO_2 catalyst-modified stainless steel substrate, which shows an extraordinary permeation behavior for an H_2/CO binary gas mixture.

2. Experimental

2.1. Sol synthesis

A colloidal silica sol and boehmite sol as intermediate layer materials were prepared to reduce the pore size of a porous stainless steel (SUS) support. The colloidal silica sol with 100 nm in particle size was synthesized from base-catalyzed hydrolysis–condensation reaction of tetraethyl orthosilicate (TEOS) purchased from Aldrich. The molar ratio of TEOS, water, ammonia and ethanol was 1:53.6:0.64:40.1. Prior to addition of a NH_3/H_2O mixture, a TEOS/ethanol mixture was stirred vigorously in an oil bath of 50 °C. The addition of the NH_3/H_2O mixture was carried out dropwise, followed by refluxing the mixture for 3 h at vigorous stirring, resulting in a stable colloidal silica sol. The boehmite sol was produced as suggested by Kusakabe et al. [18]. A polymeric silica sol was prepared under acid-catalyzed condition. A molar ratio of TEOS, water and nitric acid (purchased from Junsei) was 0.096:0.56:0.008. A mixture of TEOS, water and nitric acid was stirred at room temperature for 20 min. The reaction mixture was diluted with additional water to adjust the volume to 500 ml. After refluxing the final mixture for 8 h at 80 °C, the transparent polymeric silica sol was obtained [19].

2.2. Preparation of Pt catalysts

The as-prepared 100 nm silica xerogels, of which the specific surface area is about 84 m^2/g, were used as a support of Pt catalysts. A 3 wt.% Pt/SiO_2 catalysts were prepared via incipient-wetness impregnation with tetraammineplatinum(II) nitrate (purchased from Aldrich), followed by drying at 70 °C and calcination at 400 °C.

2.3. Preparation of composite membranes

Disks of 316L porous stainless steel (SUS) were purchased from Mott Metallurgical having a thickness of 1 mm, a surface area of 5 cm^2, and an average pore size of 0.5 μm. The porous SUS substrate was modified by the 100 nm silica xerogel or the Pt/SiO_2 catalyst. The silica xerogel or the Pt/SiO_2 catalyst was pressed into the macropores of one side of the SUS support by a press under 10 MPa, followed by calcination at 650 °C. The whole procedure of the first modification was repeated twice. The second modification of the stainless steel support was conducted by a soaking–rolling method with a boehmite sol [20]. The back side of the support loaded on the *o*-ring-sealed cell was evacuated by a rotary vacuum pump. The boehmite sol was poured onto the front side of the support, followed by maintaining vacuum of the back side of the support for 3 min so that the boehmite sol could penetrate into inner pores of the support. After the soaking process, concentrated gel layer formed on the front side of the support was rolled out with an urethane rolling pin. The modified support was dried overnight at 25 °C and calcined at 650 °C. The preparation of a top layer using the polymeric silica sol was carried out in the same manner as the support modification with the boehmite sol, and the silica top layer was dried at 25 °C and calcined at 500 °C. The prepared composite membranes are listed in Table 1.

2.4. Permeation measurement

Permeation tests were conducted with an H_2 (99%)/CO (1%) mixtures as a feed gas between 25 and 200 °C. The permeation area of the membrane was 4.52 cm^2. The flow rates of feed and sweeping He gas were 40 and 80 ml/min, respectively. The mole fractions of the permeated gases through the membrane were measured using gas chromatography with a corona ionization detector (CID), which makes it feasible to measure the extremely low concentration of CO. The parameter to describe the separation efficiency for a binary mixture is the separation factor α, which is a measure of the enrichment of a gas component after it has passed the membrane. Separation factor α is defined as

$$\alpha = \frac{y}{1-y}\,\frac{1-x}{x}$$

where x and y are the mole fraction in the feed and permeate side, respectively.

2.5. Methanol steam reforming experiments

For a methanol reforming membrane reactor, a stainless steel-supported silica membrane including Pt/SiO_2 catalysts was prepared by the soaking–rolling method and 5 g of Cu–Zn catalysts purchased from NIKKI chemical Co. was used in a whole experiment of methanol steam reforming. The methanol reforming membrane reactor system is schematically shown in Fig. 1. The methanol steam reforming experiments were carried out in the range of reaction temperature from 170 to 230 °C and feed flow rate of an H_2O/MeOH mixture with a molar ratio of 1.3 varied from 0.004 to 0.1 ml/min. The H_2O/MeOH mixture was evaporated

Table 1
Various composite membranes prepared by the soaking–rolling method

Membrane code	Composition of the layers
M1	γ-Al_2O_3/SiO_2 (100 nm)/SUS
M2	γ-Al_2O_3/Pt–SiO_2 (100 nm)/SUS
M3	SiO_2 (polymeric)/γ-Al_2O_3/SiO_2 (100 nm)/SUS
M4	SiO_2 (polymeric)/γ-Al_2O_3/Pt–SiO_2 (100 nm)/SUS

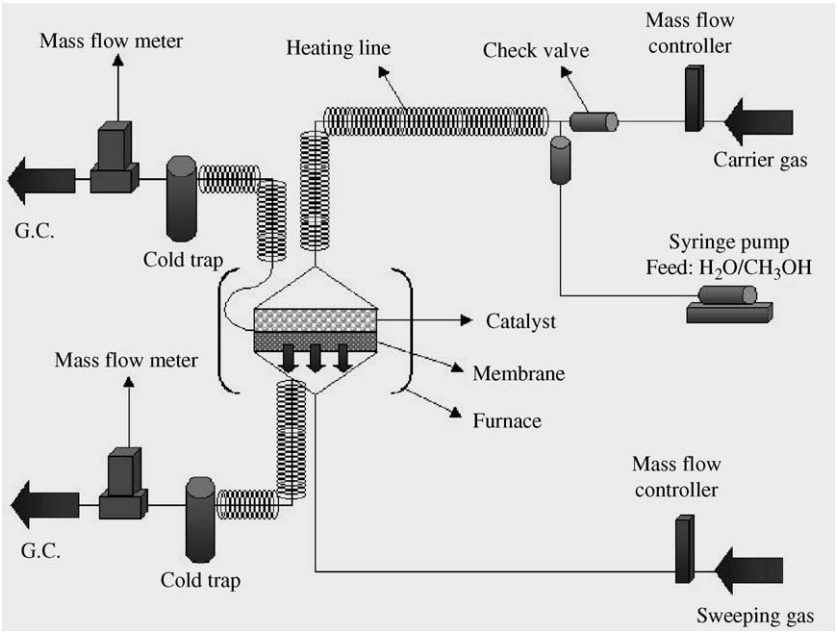

Fig. 1. Schematic diagram of the methanol steam reformer.

in a preheating line, and diluted by a carrier gas. He gas was used as a carrier gas in the feed side and as a sweeping gas in the permeate side, of which flow rates are 40 and 100 ml/min, respectively. The experiment conditions of the methanol steam reforming are summarized in Table 2. The gases permeated through the membrane were analyzed using gas chromatography with a corona ionization detector (CID). The methanol conversion in the membrane reactor was calculated from a definition described below.

$$\text{CH}_3\text{OH conversion} = \frac{\text{CH}_3\text{OH}_{\text{feed}} - \text{CH}_3\text{OH}_{\text{retentate}} - \text{CH}_3\text{OH}_{\text{permeate}}}{\text{CH}_3\text{OH}_{\text{feed}}}$$

For the confirmation of the methanol conversion improvement via the membrane reactor system, methanol steam reforming in a conventional reactor was also conducted by installing a nonporous SUS disk into the membrane reactor cell instead of the silica composite membrane.

3. Results and discussion

3.1. Permeation behavior of Pt-included composite membranes

In this study, additional CO rejection was induced by introduction of Pt/SiO_2 catalysts into an intermediate layer of a composite membrane. A γ-alumina composite membrane with and without a Pt/SiO_2 intermediate layer was synthesized to investigate the effect of Pt/SiO_2 catalysts on the CO removal efficiency. The unsupported γ-alumina, synthesized under the same conditions as in the preparation of the membrane layer, showed the average pore diameter of 4–5 nm and the BET surface area of 240 m^2/g, indicating that the Knudsen diffusion mechanism through the membrane can be expected if no serious pinholes or cracks are formed on the γ-alumina layer.

An H_2 (99%)/CO (1%) mixture permeation test of the membrane M1 was carried out to determine the separation performance of the γ-alumina layer without Pt/SiO_2 catalysts.

Table 2
Experimental conditions for the methanol steam reforming (a H_2O/CH_3OH molar ratio = 1.3, a flow rate of the He carrier = 40 ml/min)

Code	Reactor configuration	Used membrane	Feed (H_2O/CH_3OH) flow rate (ml/min)	Sweeping gas (He)
CR1	Conventional reactor	–	0.004	–
CR2	Conventional reactor	–	0.04	–
CR3	Conventional reactor	–	0.1	–
MR1	Membrane reactor	M4	0.004	100
MR2	Membrane reactor	M4	0.04	100
MR3	Membrane reactor	M4	0.1	100
MR4	Membrane reactor	M3	0.004	100
MR5	Membrane reactor	M3	0.04	100
MR6	Membrane reactor	M3	0.1	100

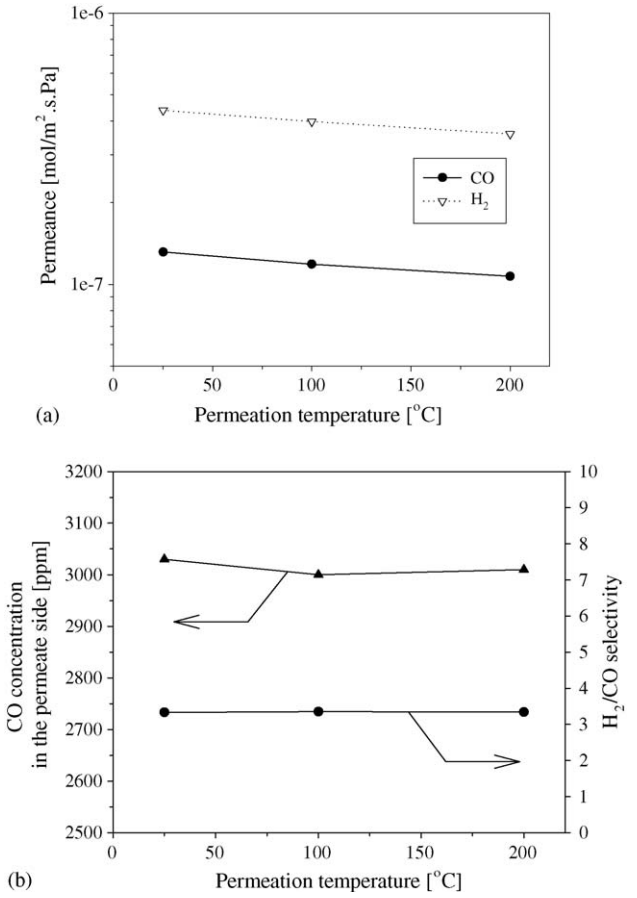

Fig. 2. Permeation results of an H_2 (99%)/CO (1%) mixture for the membrane M1: (a) H_2 and CO permeance, (b) H_2/CO selectivity and CO concentration in the permeate side.

Fig. 2a shows the temperature dependence of H_2 and CO permeances for the M1. It is revealed that the M1 with H_2 permeances and CO permeances decreased with an increase in permeation temperature. The temperature dependence of the membrane M1 is typical permeation behavior appearing in the Knudsen diffusion region [21–25]. Fig. 2b shows the H_2/CO selectivity and the CO concentration in the permeate side. The CO concentration of 10,000 ppm in the feed side of the membrane was diminished to 3000–3030 ppm in the permeate side, and the H_2/CO selectivity is about 3.4 approaching to the ideal separation factor for the pure Knudsen diffusion system. From the permeation results of the M1, it can be considered that the M1 predominantly follows the Knudsen diffusion mechanism with a little contribution of viscous flow through pinholes or cracks which can be occasionally formed on the membrane, depending on preparation conditions of the membrane. As presumed from the textural properties of the unsupported γ-alumina, the separation factor for the M1 cannot exceed the ideal separation factor for the pure Knudsen diffusion system.

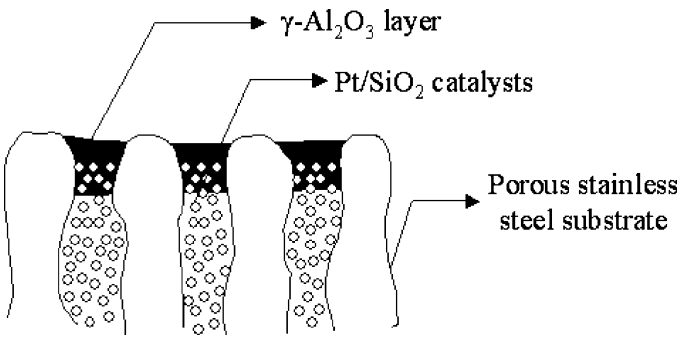

Fig. 3. Schematic diagram of the cross-sectional structure of the membrane M2.

To investigate whether the H_2/CO separation factor is improved by the introduction of Pt/SiO_2 catalysts, the Pt-included γ-alumina composite membranes, designated as M2, was prepared by the soaking–rolling method [20]. A 3 wt.% Pt catalysts supported on the silica xerogel with 100 nm in particle diameter were used to modify the porous stainless steel support. Pt/SiO_2 catalysts were pressed into pores of the substrate under 10 MPa, followed by calcination at 650 °C. The second modification of a support with the boehmite sol via the soaking–rolling method was carried out to reduce the pore size of the support into the region of Knudsen diffusion. A schematic diagram of the cross-section of the M2 shown in Fig. 3 exhibits the Pt/SiO_2 intermediate layer placed under the γ-alumina skin layer.

The permeation test of an H_2 (99%)/CO (1%) mixture between 25 and 200 °C was conducted to observe the effect of Pt catalysts, included in the membrane, on CO removal

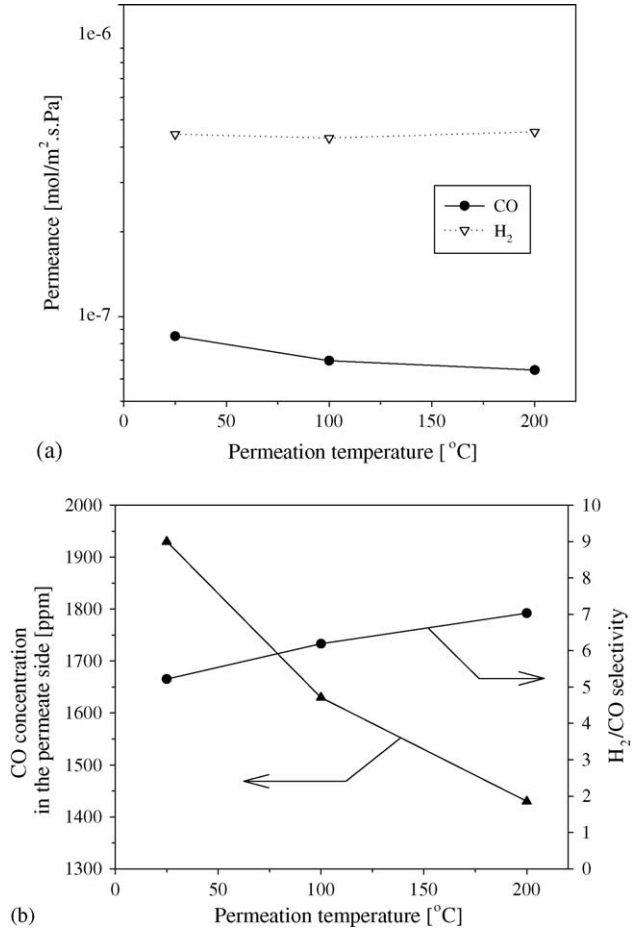

Fig. 4. Permeation results of an H_2 (99%)/CO (1%) mixture for the membrane M2: (a) H_2 and CO permeance, (b) H_2/CO selectivity and CO concentration in the permeate side.

efficiency and permeation behavior of H_2 and CO. To exclude the CO removal via CO oxidation on the Pt/SiO_2 catalysts, all of the permeation tests were carried out under oxygen-free condition using an He sweeping gas. Fig. 4a shows the temperature dependence of the H_2 and CO permeance of the membrane M2. Comparing to the permeation results of the M1, the M2 showed a little change of the H_2 permeance. However, the H_2 permeance of the M2 was unexpectedly independent of the permeation temperature despite the Knudsen-dominated pore structure of the γ-alumina layer, while the M1 showed a decrease in the H_2 permeance with an increase in permeation temperature. Fig. 4b shows the H_2/CO separation factor of the M2 and the CO concentration in the permeate side. The CO concentration of 10,000 ppm in the feed side of the membrane was reduced to 1435–1930 ppm in the permeate side, which is much lower than that for the M1, and a remarkable H_2/CO separation factor of 5.22–7.03 was obtained in the range of permeation temperature from 25 to 200 °C. Interestingly, the permeation results of the M2 exceeded the Knudsen-dominated separation behavior expected from the mesoporous γ-alumina layer. The extraordinary H_2/CO separation factor is attributed to the decrease in the CO permeance, which is derived from interaction between permeated CO and Pt catalysts in the lower side of the skin layer. In other words, considering the contribution of surface diffusion induced by the Pt catalysts placed under γ-alumina skin layer, strong interaction between CO and Pt under the skin layer leads to the decrease in the driving force of the CO permeation and allows the improvement of the H_2/CO selectivity [26]. Using the M1 and M2 as a support, silica composite membranes M3 and M4 shown in Table 1 were prepared by the soaking-rolling method, respectively. Fig. 5 presents the permeation results of an H_2 (99%)/CO (1%) binary mixture for the M3 and M4. In the case of the M4, CO was not detected in the permeate side of the membrane by the corona ionization detector (CID). From the permeation results shown in Figs. 2 and 4, it is concluded that the high CO removal efficiency of the M4 is attributed to the Pt catalysts loaded in the silica composite membrane [26].

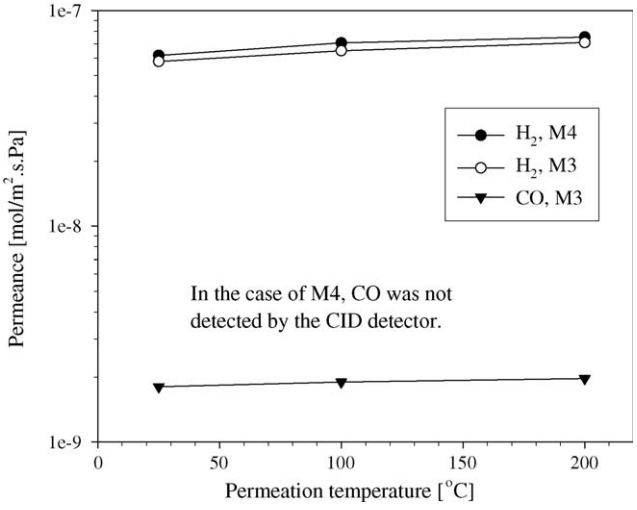

Fig. 5. Permeation results of an H_2 (99%)/CO (1%) binary mixture gas for the membranes M3 and M4 with permeation temperature.

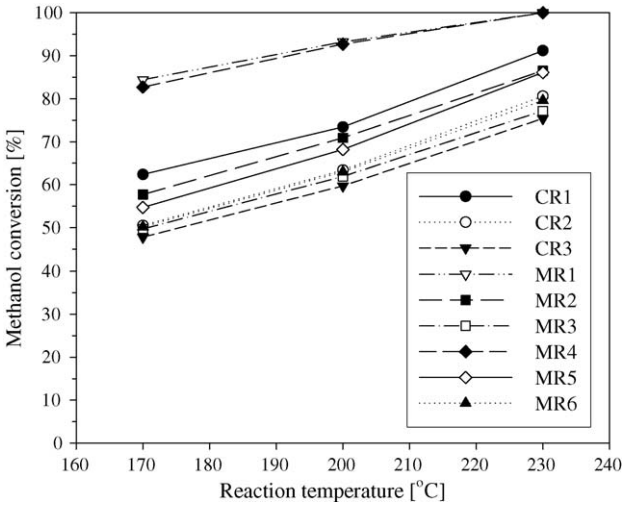

Fig. 6. Methanol conversions in the conventional reactor and the membrane reactor with different temperatures.

3.2. Methanol steam reforming membrane reactor

As shown in Table 2, the methanol steam reforming reaction was performed in a membrane reactor with the membranes M3 and M4. For the purpose of comparison, the methanol reforming experiment was also carried out in a conventional reactor without the membranes. Fig. 6 presents methanol conversions with different reactor configuration. It can be seen that, in the case of the membrane reactor, higher methanol conversions were obtained in comparison with the conventional reactor. The extent of conversion improvement observed in experiment MR1 (a difference of methanol conversion between MR1 and CR1) is almost consistent with that in experiment MR4 (a difference of methanol conversion between MR4 and CR1), due to the similar hydrogen permeance of the membrane M3 and M4 as shown in Fig. 5. It is revealed that the presence of the Pt catalysts in the membrane did not contribute to the methanol conversion. Table 3 shows the permeances of the reactants and the products measured in the permeate side of the membrane reactor. It is important to note that, in the case of the MR1, MR2 and MR3 with the membrane M4, CO was efficiently rejected through the Pt intermediate layer of the membrane M4. In contrast, MR4, MR5 and MR6 with the membrane M3 showed the CO permeances of

Table 3
Permeances and selectivities of the reactants and the products measured in the permeate side of the methanol reforming membrane reactor

Code	Permeance (nmol m^{-2} s^{-1} Pa^{-1})					H_2/H_2O	H_2/CH_3OH
	H_2	CO_2	CO	H_2O	CH_3OH		
MR1	34.0	3.10	nd[a]	3.45	1.21	9.86	28.10
MR2	31.7	2.30	nd	3.60	1.10	8.81	28.82
MR3	27.1	2.08	nd	2.97	0.92	9.12	29.46
MR4	31.2	1.92	1.43	3.14	1.05	9.94	29.71
MR5	29.4	1.56	1.25	2.92	0.98	10.07	30.00
MR6	28.9	1.45	1.12	2.81	0.94	10.28	30.74

[a] Not detected.

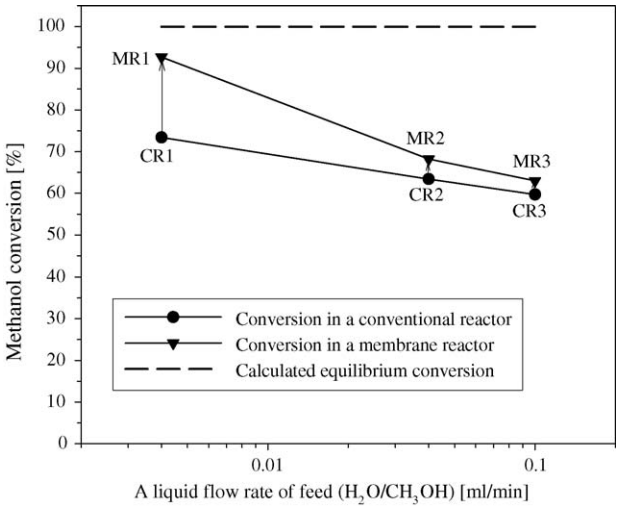

Fig. 7. Methanol conversion improvement with a decrease in an H_2O/CH_3OH feed flow rate at 200 °C.

$(1.1–1.5) \times 10^{-9}$ mol m^{-2} s^{-1} Pa^{-1}. As mentioned above, the Pt intermediate layer of the composite membrane plays a significant role in the CO removal. From Fig. 6 and Table 3, we confirmed that Pt catalysts included in the composite membrane do not affect the methanol conversion improvement, and contribute to an increase in the CO removal efficiency.

Compared with MR2, MR3, MR5 and MR6, the methanol conversions in MR1 and MR4 were considerably increased (Fig. 6). In other words, the extent of the methanol conversion improvement (a difference of methanol conversion between a membrane reactor and a conventional reactor) increased with a decrease in a H_2O/CH_3OH feed flow rate (Fig. 7), although a membrane permselectivity such as H_2/H_2O and H_2/CH_3OH was almost constant regardless of the feed flow rate (Table 3). Table 4 shows hydrogen recoveries in the methanol reforming membrane reactor. The hydrogen recovery is defined as a ratio of the permeated hydrogen to total amount of the produced hydrogen. While the hydrogen produced by the methanol steam reforming decreased with dilution of the H_2O/CH_3OH feed, the hydrogen recovery increased. A change in the extent of conversion improvement is attributed to the performance of membranes such as the hydrogen recovery, permeance and selectivity. Therefore, considering that the H_2/H_2O and H_2/CH_3OH selectivities are almost constant in all cases of MR1, MR2 and MR3 as shown in Table 3, it can be inferred that the increase in the extent of conversion improvement with feed dilution is a consequence of the increase in the hydrogen recovery.

Table 4
Hydrogen recoveries and hydrogen flow rates in the retentate side and the permeate side (permeation area of the membrane = 4.52 cm^2)

Code	Hydrogen flow rate (ml/min)		Hydrogen recovery (%)
	Retentate side	Permeate side	
MR1	0.38	0.038	9.1
MR2	5.6	0.23	3.9
MR3	11.6	0.34	2.8

However, as shown in Table 4, the increase in the hydrogen recovery via H_2O/CH_3OH feed dilution leads to a falloff in the capacity of hydrogen production. Consequently, the problem associated with the hydrogen recovery and the capacity of hydrogen production is based on the low permeance of the microporous silica composite membranes. In the case of methanol reforming membrane reactor as an energy carrier system of PEMFC, it is important to achieve both the improvement in methanol conversion and the hydrogen purification via the CO removal. Even low concentration of CO was efficiently eliminated using the microporous silica composite membranes with the Pt intermediate layer, and methanol conversion observed in experiment MR1 increased up to 20% via the dilution of H_2O/CH_3OH feed. However, in spite of the achievement of the two major objectives, total amount of the produced hydrogen was significantly low. From the viewpoint of their practical application in PEMFC system, the high capacity of hydrogen production is another crucial factor to be considered. The solution to increase the hydrogen production capacity is the mesoporous membrane reactor, because the mesoporous membranes give much higher gas permeability than the microporous membranes. However, when we use the mesoporous membranes to improve the hydrogen recovery, CO removal efficiency will considerably decrease. Therefore a different approach to eliminate CO should be used to apply the mesoporous membranes to the methanol steam reforming membrane reactor. Study on the mesoporous membrane reactor is currently underway in our laboratory.

4. Conclusions

In the methanol reforming membrane reactor system, methanol conversion was improved up to 20% in comparison with the conventional reactor, and CO was not detected in the permeate side of the membrane reactor by using the Pt-included microporous silica membranes. Compared with silica composite membranes without the Pt intermediate layer, the Pt-included microporous silica membranes showed much higher CO removal efficiency. The presence of the Pt catalysts in an intermediate layer of the membrane did not affect the methanol conversion improvement, and contributed to an increase in the CO removal efficiency. In addition, as the H_2O/CH_3OH feed flow rate decreased with the fixed flow rate of He carrier gas, the extent of the methanol conversion improvement through the membrane reactor increased due to the increase in hydrogen recovery.

References

[1] W. Donitz, Int. J. Hydrogen Energy 23 (1998) 611.
[2] L.F. Brown, Int. J. Hydrogen Energy 26 (2001) 381.
[3] J.M. Ogden, M.M. Steinbugler, T.G. Kreutz, J. Power Sources 79 (1999) 143.
[4] B. Emonts, J.B. Hansen, S.L. Jørgensen, B. Höhlein, R. Peters, J. Power Sources 71 (1998) 288–293.
[5] F. Panik, J. Power Sources 71 (1998) 36.
[6] J.C. Amphlett, R.F. Mann, B.A. Peppley, Int. J. Hydrogen Energy 21 (1996) 673.
[7] N. Itoh, Y. Kaneko, A. Igarashi, Ind. Eng. Chem. Res. 41 (2002) 4702.

[8] J.C. Amphlett, K.A.M. Creber, J.M. Davis, R.F. Mann, B.A. Peppley, D.M. Stokes, Int. J. Hydrogen Energy 19 (1994) 131.
[9] C. Lu, R.I. Masel, J. Phys. Chem. B 105 (2001) 9793.
[10] D.D. Papageorgopoulos, M. Keijzer, F.A. de Bruijn, Electrochim. Acta 48 (2002) 197.
[11] C. Lu, C. Rice, R.I. Masel, P.K. Babu, P. Waszczuk, H.S. Kim, E. Oldfield, A. Wieckowski, J. Phys. Chem. B 106 (2002) 9581.
[12] N.K. Raman, C.J. Brinker, J. Membr. Sci. 105 (1995) 273.
[13] R.M. de Vos, H. Verweij, J. Membr. Sci. 143 (1998) 37.
[14] J.C.S. Wu, H. Sabol, G.W. Smith, D.L. Flowers, P.K.T. Lin, J. Membr. Sci. 96 (1994) 275.
[15] K. Kusakabe, S. Sakamoto, T. Saie, S. Morooka, Sep. Purif. Tech. 16 (1999) 139.
[16] G.D. West, G.G. Diamond, D. Holland, M.E. Smith, M.H. Lewis, J. Membr. Sci. 203 (2002) 53.
[17] J.C.D. da Costa, G.Q. Lu, V. Rudolph, Y.S. Lin, J. Membr. Sci. 198 (2002) 9.
[18] K. Kusakabe, K. Ichiki, J.I. Hayashi, H. Maeda, S. Morooka, J. Membr. Sci. 115 (1996) 65.
[19] M. Naito, K. Nakahira, Y. Fukuda, H. Mori, J. Tsubaky, J. Membr. Sci. 129 (1997) 263.
[20] D.-W. Lee, Y.-G. Lee, B.K. Sea, S.-K. Ihm, K.-H. Lee, J. Membr. Sci. 236 (2004) 53.
[21] J.C.S. Wu, Ind. Eng. Chem. Res. 38 (1999) 4491.
[22] K.-I. Okamoto, H. Kita, K. Horii, K. Tanaka, M. Kondo, Ind. Eng. Chem. Res. 40 (2001) 163.
[23] D. Zhao, P. Yang, B.F. Chmelka, G.D. Stuky, Chem. Mater. 11 (1999) 1174.
[24] N. Nishiyama, D.H. Park, A. Koide, E.Y. gashira, K. Ueyama, J. Membr. Sci. 182 (2001) 235.
[25] D.H. Park, N. Nishiyama, Y. Egashira, K. Ueyama, Ind. Eng. Chem. Res. 40 (2001) 6105.
[26] D.-W. Lee, S.-E. Nam, B. Sea, S.-K. Ihm, K.-H. Lee, J. Membr. Sci. 243 (2004) 243.